Desalination and Water Treatment
www.deswater.com

doi: 10.1080/19443994.2016.1164084

57 (2016) 26448–26460
November

Taylor & Francis
Taylor & Francis Group

Adsorptive removal of *p*-nitroaniline from aqueous solution by bamboo charcoal: kinetics, isotherms, thermodynamics, and mechanisms

Guangqian Wu[a,*], Guannan Wu[b], Qisheng Zhang[c]

[a]*College of Biology and Environment, Nanjing Forestry University, Nanjing 210037, China, Tel. +86 25 85427133, +86 138 1387 7965; Fax: +86 25 85427061; email: kdwu@163.com*
[b]*School of Graduates, Hong Kong Baptist University, Hong Kong 999077, China, Tel. +86 136 1327 7005; Fax: +86 2554783344; email: wgnkb24111@vip.qq.com*
[c]*College of Wood Science and Technology, Nanjing Forestry University, Nanjing 210037, China, Tel. +86 136 0517 0544; Fax: +86 25 85427065; email: zhangqs@njfu.edu.cn*

Received 2 December 2015; Accepted 6 March 2016

ABSTRACT

The characteristics of commercial bamboo charcoal and adsorptive removal of *p*-nitroaniline (PNA) from aqueous solution by this bamboo charcoal were studied intensively. The effects of adsorbent grain size and solution pH value on the adsorption were investigated by conducting a series of batch adsorption experiments. The results showed that bamboo charcoal with grain size of 80–100 mesh was optimal for the adsorption, and the removal efficiency kept decreasing with the increase of solution pH value, the acidic solution environment was generally optimal for this adsorption. The adsorption amount decreased with increasing solution temperature, and the maximum adsorption amount of PNA (C_0 = 400 mg/L) was found to be 176.92 mg/L (278 K), 170.10 mg/L (298 K), and 154.93 mg/L (308 K), respectively. The kinetic rates were modeled by using the pseudo-first and pseudo-second-order equations, and the pseudo-second-order equation could explain the adsorption kinetics most effectively. The equilibrium data were fitted with the Langmuir, Freundlich, Redlich–Peterson, and Dubinin–Radushkevich models, and the result showed it followed the Redlich–Peterson model very well, which suggested the co-existence of single-layer adsorption and heterogeneity of adsorption mechanisms. The thermodynamic data showed the adsorption was a spontaneous and exothermic process. The entropy of the adsorption was greater than zero, which suggested the net increase of system randomness.

Keywords: Bamboo charcoal; Adsorption; Nitroaniline; Kinetics; Isotherm

1. Introduction

Bamboo charcoal is usually made from bamboo culms, branches, and roots, which are usually taken from bamboo plants (five years or older) and are pyrolyzed in oxygen-free or oxygen-limiting circumstance at temperatures over 700–1,200℃. It has been proven to be an environmentally functional, low cost and renewable bioresource with high surface area and excellent adsorption properties [1,2]. In recent years, the excellent adsorption properties of bamboo charcoal and its application in removal of toxic organic

*Corresponding author.

compounds in surface and drinking water have been widely investigated [1–9].

The *p*-nitroaniline (PNA) is a bright yellow, needle-like crystalline solid having the formula $C_6H_6N_2O_2$, molecular weight of 138.12, density of 1.424(20/4°C), and pK_a of 1.00. It is an organic chemical compound, consisting of a phenyl group attached to an amino group which is para to a nitro group. This chemical is commonly used as an intermediate in the synthesis of dyes, antioxidants, pharmaceuticals, and gasoline. However, PNA is usually classified as a type of hazardous substance, and can cause long-term damage to the environment. In consideration of the huge threat of PNA to the environment, this compound has been officially included in the *Black List of water environmental preferred controlled pollutants* by Ministry of Environmental Protection of China in 1989 [10]. The discharge limit for PNA-containing water is also very stringent in China, which is less than 1.0 mg/L in Chinese National Standard GB 8978–1996 [11].

Consequently, the effective removal of PNA in surface and drinking water is quite important for water quality improvement, and it is also a big challenge to environmental engineers. Currently, the PNA-containing wastewater is usually treated by photo-catalysis [12,13], biodegradation [14,15], advanced oxidation [16], and adsorption [17–20]. Among these technologies, adsorption has been proven to be effective and convenient in separating PNA from various water bodies. Different types of adsorbents have been investigated and utilized to remove PNA, such as activated carbon fiber [18], polymeric adsorbents [19,20], and carbon nanotube [21].

In recent years, bamboo charcoal has received increasing attention in the field of environmental purification, and a great number of studies have been performed over the last decade to investigate the adsorption properties of various organic compounds onto bamboo charcoal [22–25]. However, to the best of our knowledge, the adsorption of PNA on bamboo charcoal had not been investigated in previous studies and in this paper, the key characteristics of commercial bamboo charcoal, including the surface morphology, functional groups, specific surface area, and pore size distribution were investigated to elucidate the adsorption process of PNA on bamboo charcoal surface, and the kinetics, isotherms, and thermodynamics of this adsorption process were also discussed using various models. The goal of this study was to obtain a clear and comprehensive understanding of the adsorption process of PNA onto bamboo charcoal.

2. Material and methods

2.1. Materials

The commercial bamboo charcoal was provided by Zhongzhu Bamboo Charcoal Industry Co., Ltd (Anji, China). Firstly, this bamboo charcoal sample was finely ground and sieved to different meshes (6–10, 10–16, 60–80, 80–100, 100–200 meshes), after having been washed in copious amount of deionized water, they were dried in sun to eliminate moisture and were stored in desiccators. PNA (AR grade) was purchased from Sinopharm Chemical Reagent Co., Ltd (Shanghai, China). The deionized water was produced by an Ultra-pure UV Water System manufactured by Hi-tech Instruments Co., Ltd (Shanghai, China). All of the other chemicals were of AR grade and were used without further purification.

2.2. Analytical methods

All solutions used in this experiment were buffered to needed pH values with a mixture of sodium dihydrogen phosphate and disodium hydrogen phosphate ($NaH_2PO_4 + Na_2HPO_4$, ion strength = 10 mM), the detailed buffer composition is provided online [26], and the actual pH values of these buffered solution were double-checked and compared with their theoretical values, the comparison showed these two values were quite close, which demonstrated the reliability of these buffer compositions.

Concentration of PNA in this experiment was determined by an UV–vis spectrophotometer (TU-1810, P-General Instrument Co., Ltd, China) according to the method provided by literature [27], which was based on the measurement of maximum absorbance at λ_{max} = 380 nm, and the absorbance is proportional to the aqueous PNA concentration. The calibration curve of PNA was also determined using the same method and the correlation coefficient R^2 was 0.9978.

The surface morphology of bamboo charcoal was observed by using scanning electron microscopy (SEM, Quanta-200, FEI Company, USA). The surface area and porosity were determined by N_2 adsorption at 77 K with surface area and porosimetry analyzer (ASAP 2020, Micromeritics Corp, USA). The X-ray photoelectron spectroscopy (XPS) measurement was carried out with a Kratos AXIS Ultra DLD system (Rigaku Corporation, Japan). The other instruments used in this study were an acid meter (PHS-3C, Kangyi Instruments, China) and an incubator shaker (HZP-250, Jionghong Instruments, China).

2.3. Batch adsorption experiments

The batch adsorption experiments were carried out in a series of 50 mL capped Teflon bottles where 0.1 g bamboo charcoal sample and 50 mL of PNA buffered solution (25–500 mg/L) were added with no headspace in these bottles. Then, these sealed bottles were placed into a temperature-controlled incubator shaker, which was set to a fixed speed of 100 rpm and fixed temperature points of 278, 298, and 308 K.

After the adsorption, water samples in these bottles were centrifuged at 4,000 rpm and then were filtered rapidly through 0.45 μm membranes (equipped with 33 mm diameter syringe filter, Thermo Scientific Inc.), the filtrates were tested immediately on the UV–vis spectrophotometer to determine the equilibrium concentrations of PNA.

The adsorbed amount of PNA (q_e, mg/g) was calculated using Eq. (1):

$$q_e = \frac{(C_0 - C_e)V}{m} \tag{1}$$

where C_0 and C_e (mg/L) are the initial and equilibrium concentrations of PNA, respectively; V (L) is the volume of PNA solution, 50 mL; m (g) is the mass of bamboo charcoal, 0.1 g.

To determine the best-fit model for the adsorption process, the nonlinear curve fitting facility of Origin 8.5 (Origin Lab Corporation, USA) was employed to evaluate the fitting of different models. To compare the validity of each model, a normalized standard deviation Δq_e (%) was calculated using Eq. (2):

$$\Delta q_e(\%) = 100\sqrt{\frac{\sum_{i}^{N}\left[(q_{i,exp} - q_{i,cal})/q_{i,exp}\right]^2}{(N-1)}} \tag{2}$$

where N is the total number of data points and i is the serial number of each data point; $q_{i,exp}$ (mg/g) and $q_{i,cal}$ (mg/g) are the experimental and calculated adsorption amount of PNA at each data point.

3. Results and discussion

3.1. Characterization of bamboo charcoal

The SEM image of bamboo charcoal sample was shown in Fig. 1(a) and (b). As could be seen in these figures, the bamboo charcoal kept nearly the original morpha of raw bamboo, a sponge-like structure was clearly found on the cross section of bamboo charcoal, this structure was quite different from those of other carbonaceous adsorbents, such as various nutshell ACs or ACFs. The size of these small cells on the cross section always ranged from several to dozens of micrometers according to the scale on Fig. 1(a) and (b). Numerous pores, including the micro-, meso-, and macropores, were distributed in the internal wall of these small cells. These pores, accompanied with numerous wrinkles and cracks, contributed most to the total surface area of bamboo charcoal. It is generally believed that this unique sponge-like structure of bamboo charcoal originated from the intrinsic vascular bundles and parenchyma tissues of raw bamboo [28], which are the main constituents of the central cylinder of the internodes. In the pyrolysis process, all of the organic contents in these vascular bundles and parenchyma tissues, such as lignin, cellulose, and hemicellulose were decomposed and vaporized completely, and then the resulting sponge-like structure was left.

The curves of N_2 adsorption/desorption and pore size distribution of bamboo charcoal were shown in Fig. 2(a) and (b). The shape of this adsorption/desorption curve was a mixture of type I and IV isotherms in the IUPAC classification, with a quite narrow hysteresis loop at high relative pressure area. It is generally believed that the formation of hysteresis loop is mainly due to differences in curvature of the meniscus on adsorption (cylindrical) and desorption (spherical), so the occurrence of narrow hysteresis loop on this curve definitely suggested the existence of mesoporous structure on bamboo charcoal surface. Fig. 2(b) showed a vast majority of pores fell into the width less than 25 nm, suggesting a mixed micro- and mesoporous porosity of bamboo charcoal. The structure parameters, including BET surface area, pore volume, and average pore width were summarized in Table 1.

The XPS survey spectrum exhibited prominent peaks due to different surface element, consequently, the high resolution XPS measurement was employed to detect the possible elements on bamboo charcoal surface, which was showed in Fig. 3(a), (b), and (c). In Fig. 3(a), the peaks of C1s, O1s, and Na1s were acquired over 282–294, 524–544 eV, and 970–990 eV, respectively. It was very interesting that the N1s peak was totally missing in this spectrum, which indicated the nitrogen content on bamboo charcoal surface was so tiny that the instrument cannot clearly detected it; this result was quite different from the XPS spectra of activated carbons presented in other literature [29–31], which always revealed a tiny but very clear N1s peak at around 400 eV. Another interesting point of Fig. 3(a) was the occurrence of Na1s at around 980 eV, the Na1s peak in the survey spectrum was quite clear, which indicated the Na atom might widely spread on bamboo charcoal surface. However, the Na1s peak

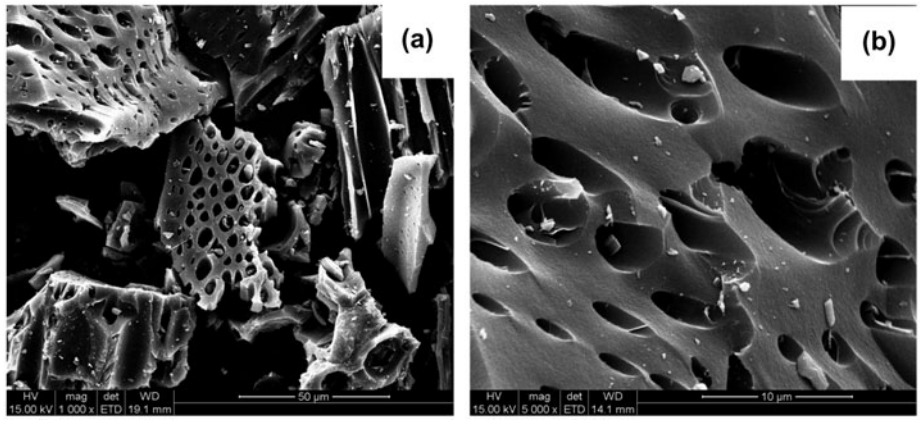

Fig. 1. The SEM images of bamboo charcoal with different magnification ((a) 1,000× and (b) 5,000×).

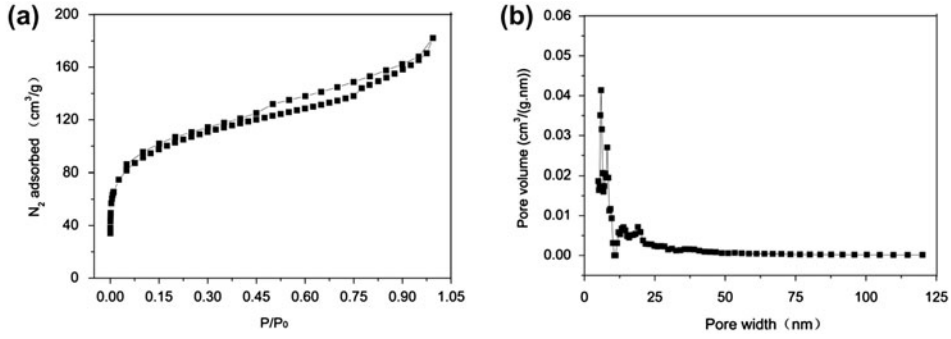

Fig. 2. The curves of N_2 adsorption/desorption and pore size distribution of bamboo charcoal ((a) N_2 adsorption/desorption curve and (b) pore size distribution curve).

Table 1
The porosity parameters of experimental bamboo charcoal

Bamboo charcoal	Specific surface area (m^2/g)	Average pore width (nm)	Total pore volume (cm^3/g)	Micropore volume (cm^3/g)	Surface area of micropore (m^2/g)
	321.45	16.61	0.282	0.123	236.47

could hardly be found on the XPS spectrum of conventional activated carbons, so the relatively high Na content on bamboo charcoal surface might suggest the high capacity of bamboo tissue to absorb and accumulate Na element from soil.

In this part, the Origin 8.5 was employed to integrate the peak area of C1s, O1s, and Na1s, to get the relative C, O, and Na content on bamboo charcoal surface. The result showed the relative content of C atom was 72.21%, while those of O atoms and Na atoms were 18.62 and 9.17%, respectively. So it was quite clear that the C atoms were dominant on the bamboo charcoal surface, and the O atoms were usually fixed with C atoms to form various functional groups.

The XPS survey spectrum of bamboo charcoal was further measured to give quantitative content of surface functional groups, so the C1s and O1s peaks were deconvolved to some sub-peaks, as shown in Fig. 3(b) and (c). Fig. 3(b) presented several carbon species and the optimum fitting was achieved by deconvolution of six peaks for the C1s spectrum: graphitic or aromatic carbon (C–C, 284.5 eV and C=C, 285.0 eV), carbon present in phenolic, alcohol, and ether groups (C–O, 285.5 eV), carbonyl groups (C=O, 287.8 eV), carboxyl,

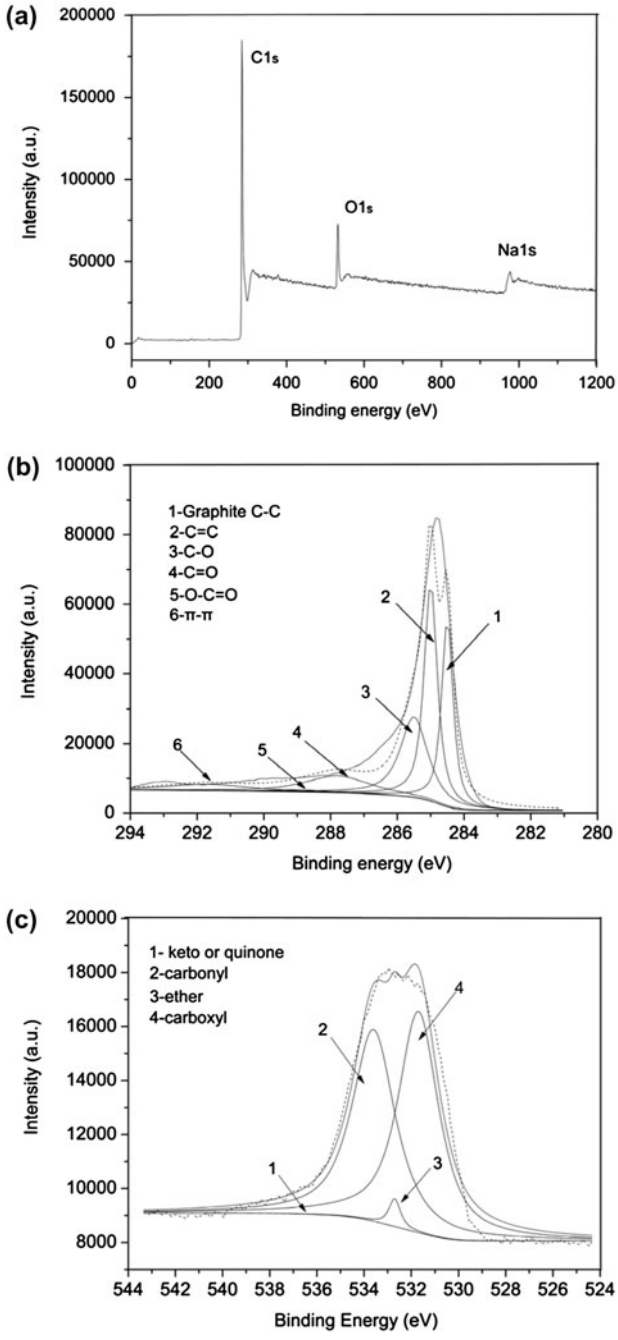

Fig. 3. The XPS survey spectrum and fitting curves of C1s and O1s ((a) XPS survey spectrum, (b) XPS fitting curve of C1s, and (c) XPS fitting curve of O1s).

lactone, or ether groups (O=C–O, 288.9 eV), and shake-up satellite peaks due to π–π transition in aromatic rings (291.7 eV). Fig. 3(c) presented the oxygen species on the surface of bamboo charcoal, four different oxygen-containing functional groups were identified, as reported by Kodama [32]: oxygen atoms in keto and quinone groups (C=O, 529.5 eV), carbonyl oxygen atoms in esters, amides, and anhydrides as well as oxygen atoms in hydroxyls or ethers (531.7 eV), ether oxygen atoms in esters and anhydrides (532.7 eV), and oxygen atoms in the carboxyl groups (533.6 eV).The relative content of each functional group was obtained from the area of sub-peaks divided by the total area, which was shown in Table 2. It was clear that the graphitic or aromatic carbon atoms were dominant in the total carbon composition, and most of the oxygen atoms were fixed into the carbonyl and carboxyl groups.

3.2. Effect of bamboo charcoal grain size on adsorption

In this experiment, five different grain size, 6–10, 10–16, 60–80, 80–100, and 100–200 meshes, were prepared to compare their adsorption capacities for PNA, the result was shown in Fig. 4. It could be easily found that the solution pH values kept nearly constant during the adsorption process, and the removal efficiency kept increasing with the decrease of grain size, which indicated smaller bamboo charcoal grain size was beneficial to the adsorption. However, the removal efficiency began to keep nearly constant when the grain size was less than 80–100 mesh. In consideration of the operation factor in pilot or field application, too small adsorbent grain size would inevitably cause some difficulties to the operators or to the devices, such as the pipe clogging or device damage, so the proper selection of adsorbent grain size is one of the key factors in practical application. In this experiment, the grain size of 80–100 mesh could obtain the almost best removal efficiency, and could also facilitate the operation, so the bamboo charcoal sample with grain size of 80–100 mesh was used in the following experiment to evaluate the adsorption performance.

3.3. Effect of solution pH on adsorption

In this experiment, a series of PNA solutions with various pH values (2.0–10.0) were prepared to investigate the relation of adsorption capacities and solution pH values, the result was shown in Fig. 5. It was obvious that the removal efficiency decreased with the increase of solution pH values. However, the decrease rate was quite slow within the pH range 2.0–7.0, and it became much more rapid when the solution pH exceeded 7.0, this phenomenon apparently suggested that the acidic solution environment was generally optimal to the adsorption, while the basic solution environment would deteriorate the adsorption dramatically.

Table 2
The C1s and O1s deconvolution and peak area of experimental bamboo charcoal

Element	C1s						O1s			
BE (eV)	284.5	285.0	285.5	287.8	288.9	291.7	529.5	531.7	532.7	533.6
Functional groups	C–C	C=C	C–O	C=O	O–C=O	π–π	Keto/Quinone	Carbonyl	Ether	Carboxyl
Peak area	33,575	51,986	12,019	21,607	12,058	7,359	<1	24,466	887	22,578
%	24.22%	37.51%	8.67%	15.59%	8.70%	5.31%	0	51.04%	1.86%	47.10%

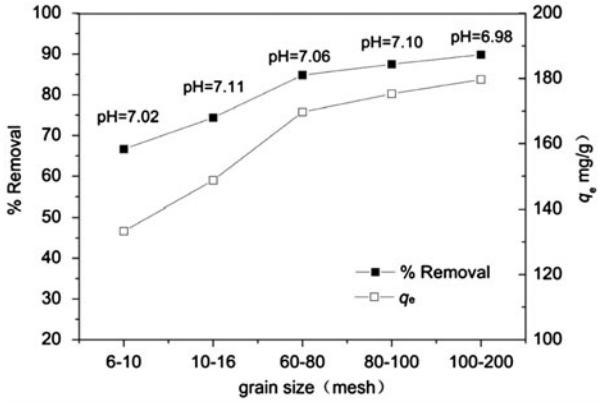

Fig. 4. The effect of bamboo charcoal grain size on adsorption (C_0 = 400 mg/L; T = 298 K; bamboo charcoal mass = 0.1 g; solution pH 7.0).

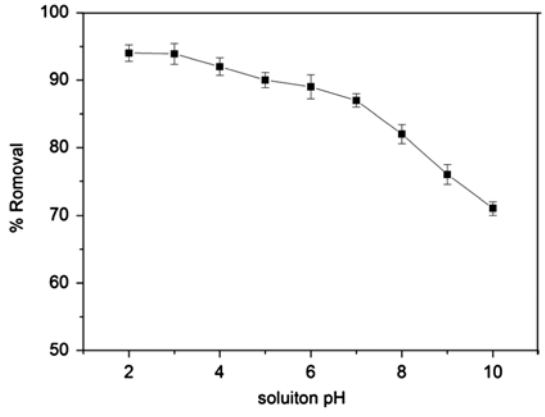

Fig. 5. The effect of solution pH on adsorption (C_0 = 400 mg/L; T = 298 K; bamboo charcoal mass = 0.1 g, solution pH 2.0–10.0).

It is generally believed that five different forces: the Van der Waals force, hydrogen bond interaction, electron donor–acceptor interaction, electrostatic force, and conjugated π–π interaction were involved in solid/liquid phase adsorption [33]. Within these forces, the Van der Waals force, electron donor–acceptor interaction, and the conjugated π-π interaction were mainly determined by the intrinsic properties of PNA molecules and adsorption sites on bamboo charcoal surface, such as the molecular or atomic weight, distance between different molecules or atoms, and the valence electrons in the atomic orbit, so these forces would not be heavily affected by the solution pH. Consequently, the dramatic decrease of removal efficiency, especially in the basic solutions, could be clearly attributed to the combined effects of hydrogen bond interaction and electrostatic force between adsorbent and adsorbate.

In aqueous solution, the existing form of PNA could change rapidly under different pH values, and the equations could be expressed as follows:

$$C_6H_4NO_2NH_3^+ \Longleftrightarrow C_6H_4NO_2NH_2 + H^+$$

$$pH = pK_a + \log [C_6H_4NO_2NH_2]/[C_6H_4NO_2NH_3^+]$$

$$\log[C_6H_4NO_2NH_2]/[C_6H_4NO_2NH_3^+] = pH - pK_a$$

When $pH - pK_a > 0$, $[C_6H_4NO_2NH_2]/[C_6H_4NO_2NH_3^+] > 1$, so most of the PNA in the aqueous solution is in the form of electron-neutral PNA molecules. When $pH - pK_a < 0$, $[C_6H_4NO_2NH_2]/[C_6H_4NO_2NH_3^+] < 1$, the positively charged PNA ions is dominant in the aqueous solution.

Literature [34] said that when the solution pH values is within $pK_a \pm 2.0$, the electron-neutral molecules and positively charged ions can co-exist in aqueous solution, while the solution pH values exceed this limits, the electron-neutral molecule or the positively charged ions will be dominant solely in aqueous solution, which was summarized in Table 3.

Previous research showed the point zero charge (pH_{pzc}) of bamboo charcoal in this experiment was 8.71 [35], which suggested that the bamboo charcoal surface would be fully positively charged within experimental solution pH 2.0–8.0, and there were also some positively charged PNA ions within experimental solution pH 2.0–3.0 (Table 3), so the electrostatic repulsion force played a key role in deteriorating the

Table 3
The form of PNA molecule in aqueous solution with different pH values

Solution pH values	Existing form
≦1.0	Positively charged PNA ions
1.0–3.0	Electron-neutral PNA molecules and a few of Positively charged PNA ions co-exist in solution, and percentage of electron-neutral PNA molecules keeps increasing with the increase of solution pH value
>3.0	Electron-neutral PNA molecules

adsorption in this solution pH range. When the solution pH exceeded 3.0, the positively charged bamboo charcoal surface would have no interaction with the electron–neutral PNA molecules (Table 3), so the electrostatic force could be totally omitted when solution pH exceeded 3.0. Another important force involved in this adsorption process was hydrogen bond interaction. It was generally believed that some hydrogen or oxygen-containing groups, especially the carbonyl and carboxyl were involved in this interaction [32–35]. The XPS analysis in Table 2 also showed the dominant role of carbonyl and carboxyl in the total group composition, and with the continuous increasing of solution pH values, an increasing number of carboxyl would be dissociated to ion state, consequently, the strength of hydrogen bond interaction between carboxyl and PNA molecules would be inevitably decreased and would be totally missing when solution pH exceeded 7.0. However, the carbonyl could keep stable in the aqueous solution and the strength of hydrogen bond interaction between carbonyl and PNA molecules could keep nearly constant despite the increase of solution pH. The combined effect of these forces on the adsorption was summarized in Table 4.

3.4. Adsorption kinetics

The effect of contact time on adsorption was showed in Fig. 6. It could be found that the adsorption amounts of PNA increased gradually with the rise of contact time until q_t remained invariable. The adsorption equilibrium of PNA on bamboo charcoal could be reached within 300 min, and more than 80 percent of the equilibrium adsorption amounts could be obtained within the initial 120 min. The equilibrium adsorption amount of PNA was 176.92 mg/L (278 K), 170.10 mg/L (298 K), and 154.93 mg/L (308 K), respectively, with the initial concentration of 400 mg/L. Fig. 6 also showed the adsorption of PNA onto bamboo charcoal surface was easily affected by the variation of solution temperature, and lower temperature was always beneficial to the adsorption.

As is mentioned above, the adsorption process of PNA molecule onto bamboo charcoal was mainly dominated by various physical forces, and in some ways, the solid/liquid phase adsorption functioned mainly by physical forces could be seemed as the "condensation" of free adsorbate molecule on adsorbent surface. With the increase of solution temperature, the irregular

Table 4
The forces between PNA molecule and bamboo charcoal under different solution pH values

Solution pH values	2.0	3.0	4.0	5.0	6.0	7.0	8.0	9.0	10.0
Van Der Waals force	Unchanged								
Electrostatic interaction	Strong repulsion	Weak repulsion	Nearly neutral	Neutral	Neutral	Neutral	Neutral	Neutral	Neutral
Hydrogen bond interaction caused by carboxyl	Strong	Strong	Strong	Strong	Weak	Very weak	Extremely weak	Extremely weak	Extremely weak
Hydrogen bond interaction caused by carbonyl	Strong	Strong	Strong	Strong	Strong	Strong	Strong	Strong	Strong
Electron donor–acceptor interaction	Unchanged								
Conjugated π–π interaction	Unchanged								

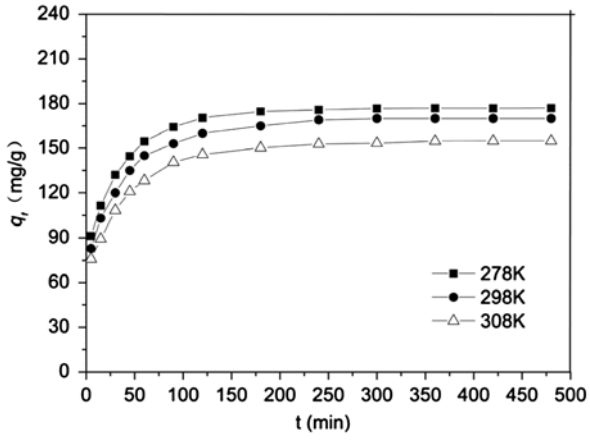

Fig. 6. The kinetic rates of this adsorption process (C_0 = 400 mg/L; bamboo charcoal mass = 0.1 g; solution pH 7.0).

Brownian Motion of H_2O molecule became increasingly vigorous, and the impact of moving H_2O molecule would inevitably disturb the transfer of PNA molecule from bulk solution to bamboo charcoal surface and re-entrain the adsorbed PNA molecule back to the bulk solution, so the equilibrium adsorption amount decreased dramatically with the increase of solution temperature.

In order to investigate the adsorption processes of PNA on bamboo charcoal, kinetic analyses were usually conducted using pseudo-first-order and pseudo-second-order models. The equation of pseudo-first-order model could be expressed as follows:

$$\log(q_{e,cal} - q_t) = \log q_{e,cal} - \frac{k_1 t}{2.303} \quad (3)$$

The equation of pseudo-second-order model could be expressed as follows:

$$\frac{t}{q_t} = \frac{1}{k_2 q_{e,cal}^2} + \frac{t}{q_{e,cal}} \quad (4)$$

where $q_{e,cal}$ (mg/g) is the calculated equilibrium amount of PNA adsorbed on bamboo charcoal using these two models; q_t (mg/g) is the amount of PNA adsorbed on bamboo charcoal at time t (min); k_1 (1/min) is the rate constant of pseudo-first-order model; k_2 (g/(mg min)) is the rate constant of pseudo-second-order model.

The regression curves of pseudo-first-order and pseudo-second-order model were also shown in Fig. 7(a) and (b), and the corresponding kinetic parameters were listed in Table 5.

As seen from Fig. 7(a) and (b), the pseudo-first-order model did not show a good agreement with the kinetic data, which could also be concluded from the lower correlation coefficients (R^2 = 0.9877, 0.9835, and 0.9723) and larger normalized standard deviation Δq_e (20.17, 19.84, and 17.95%) listed in Table 5. However, the pseudo-second-order model fitted the experimental data very well, and the correlation coefficients (R^2) and the normalized standard deviation (Δq_e) were quite satisfied. Therefore, the pseudo-second-order model was suitable to describe this kinetic process.

3.5. Adsorption isotherm

In this study, the equilibrium data was analyzed using the well-known isotherm models of Langmuir, Freundlich, Redlich–Peterson, and Dubinin–Radushkevich. It is generally believed that the Langmuir model could describe quantitatively the formation of a monolayer adsorbate on the outer adsorbent surface, and after that, no further adsorption takes place. Furthermore, the surface of adsorbent should be homogeneous, which means the adsorption mechanism at each adsorption site is similar to the others [1–9,35]. The Freundlich model is commonly used to describe the adsorption characteristics for the heterogeneous surface, the "Heterogeneity" always means the difference of porosity and the adsorption mechanism [35]. The Redlich–Peterson model incorporates the features of both the Langmuir and Freundlich models [34,35]. It considers the heterogeneous adsorption surface in Freundlich model and the possibility of single layer adsorption in Langmuir model. The Dubinin–Radushkevich model is generally applied to express the adsorption mechanism with a Gaussian energy distribution onto a heterogeneous surface. This model has often successfully fitted high solute activities and the intermediate range of concentrations data well. These isotherm equations are given in Table 6.

Fig. 8(a), (b), and (c) showed the regression curves of four types of isotherm models under different temperature. All of the parameters obtained from these models were shown in Table 7. By comparing the correlation coefficients of these isotherm models at different temperatures, it was clear that the equilibrium data of three temperature could be best fitted by Redlich–Peterson model (the correlation coefficients were 0.9964, 0.9952, and 0.9882, respectively), and the values of Δq_e of Redlich–Peterson model listed in Table 7 were quite smaller than those of the other models.

As mentioned above, the Redlich–Peterson model is generally seemed as the combination of Langmuir and Freundlich model, which always notify the

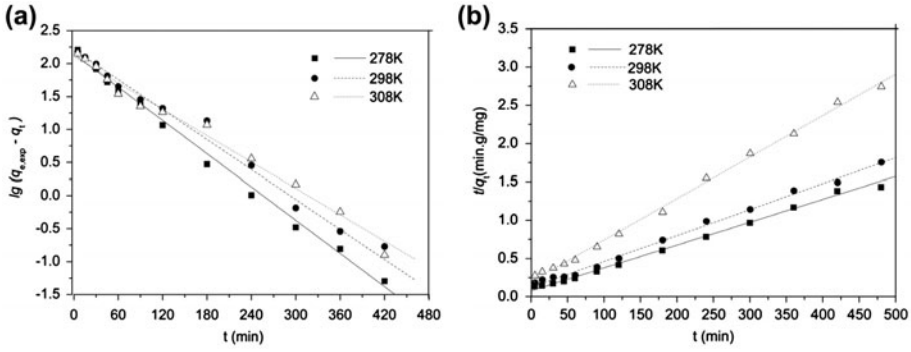

Fig. 7. The kinetic model fitting curves of this adsorption process ((a) pseudo-first-order model and (b) pseudo-second-order model; C_0 = 400 mg/L; bamboo charcoal mass = 0.1 g; solution pH 7.0).

Table 5
Kinetic parameters for adsorption of PNA onto bamboo charcoal

	T (K)		
Parameter	278 K	298 K	308 K
Pseudo-first-order model			
R^2	0.9877	0.9835	0.9723
$q_{e,exp}$ (mg/g)	176.92	170.10	154.93
$q_{e,cal}$ (mg/g)	139.44	162.52	126.77
Δq_e (%)	20.17	19.84	17.95
k_1 (1/min)	1.935×10^{-2}	1.750×10^{-2}	1.543×10^{-2}
Pseudo-second-order model			
R^2	0.9999	0.9989	0.9995
$q_{e,exp}$ (mg/g)	176.92	170.10	154.93
$q_{e,cal}$ (mg/g)	196.07	185.19	172.41
Δq_e (%)	10.70	11.42	10.56
k_2 (g/(mg min))	1.436×10^{-4}	1.403×10^{-4}	1.255×10^{-4}

adsorption behavior has both the characteristics of monolayer and surface heterogeneity, and the forces or mechanisms involved in adsorption are also complex. As for the bamboo charcoal, the SEM images demonstrated the complex porosity inside the bamboo charcoal and the XPS spectrum also showed us the existence of various functional groups on bamboo charcoal surface, so the heterogeneity of bamboo charcoal surface was quite easy to be understood. However, it was also quite understandable that the contribution of each force or mechanism to the adsorption was quite different, and one or more forces or mechanisms would inevitably play a more important role in adsorption than the other forces or mechanisms.

3.6. Thermodynamic study

Thermodynamic parameters were evaluated to confirm the nature of PNA adsorption on bamboo

Table 6
Isotherm equations and the parameters

Isotherm	Equation	Parameters
Langmuir	$q_e = \frac{C_e K_L q_{max}}{1 + C_e K_L}$	Q_e: equilibrium adsorption amount of PNA(mg/g); C_e: equilibrium concentration of PNA (mg/L); q_{max}: maximum monolayer adsorption amount of PNA (mg/g); K_L: Langmuir constant (L/mg)
Freundlich	$q_e = K_F C_e^{\frac{1}{n}}$	K_F: Freundlich constant (mg/g (L/mg)$^{1/n}$); $1/n$: related to the magnitude of the adsorption driving force and to the adsorbent site energy distribution
Redlich–Peterson	$q_e = \frac{aC_e}{1 + bC_e^c}$	a, b: Redlich–Peterson model constants; c: the Redlich–Peterson model exponent reflecting the heterogeneity of the adsorbent
Dubinin–Radushkevich	$q_e = q_D \exp[-B_{DR}(RT \ln(1 + 1/C_e)]$	B_{DR}: related to the free energy of adsorption per mole of the adsorbate as it migrates to the surface of the adsorbent from infinite distance in the solution (mol^2/kJ^2); q_D: the Dubinin–Radushkevich theoretical isotherm saturation capacity (mg/g)

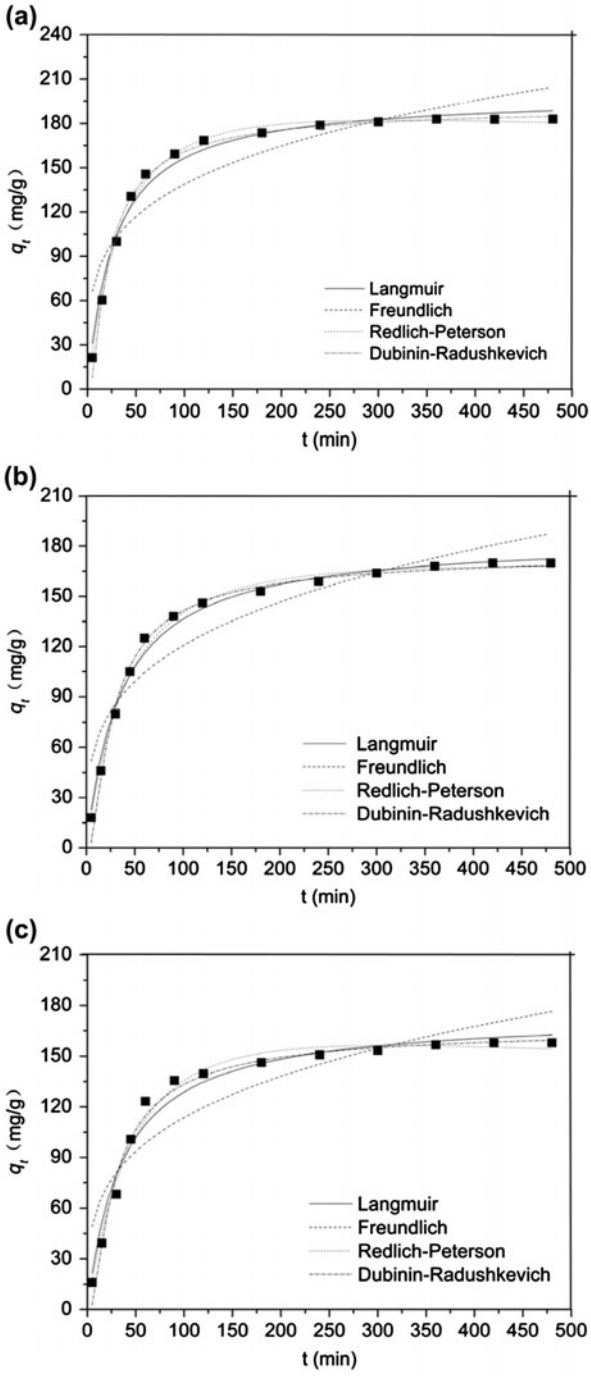

Fig. 8. The fitting curves of four different isotherm model under three temperatures ((a) 278 K, (b) 298 K, and (c) 308 K; C_0 = 25–500 mg/L; bamboo charcoal mass = 0.1 g; solution pH 7.0).

charcoal. The thermodynamic parameters, including the Gibbs free energy change (ΔG°), enthalpy change (ΔH°), and entropy change (ΔS°), were calculated to evaluate the thermodynamic feasibility and spontaneous nature of this process. These parameters were calculated from the variation of the thermodynamic equilibrium constant K_0 with respect to temperature [36]. K_0 for the adsorption reaction can be defined as follows [37]:

$$K_0 = \frac{C_s/C_s^0}{C_e/C_e^0} \tag{5}$$

where C_s is the surface concentration of PNA in mole per gram of bamboo charcoal (mol/g), C_e is the aqueous concentration of PNA at equilibrium (mol/l), C_s^0 is the surface concentration of PNA at monolayer coverage of the adsorbent (mol/m^2), C_e^0 is molar concentration of PNA at standard condition and is equal to 1 M. The standard free energy change (ΔG°) for adsorption was calculated from the following relationship:

$$\Delta G^\circ = -RT\ln(K_0) \tag{6}$$

where R is the universal gas constant and T is the temperature in Kelvin. Using the Van't Hoff equation [38], the average standard enthalpy change (ΔH°) can be calculated from the relationship between K_0 and T:

$$\ln K_0 = -\Delta H^\circ/RT + \text{const} \tag{7}$$

and standard entropy changes (ΔS°) can be calculated from:

$$\Delta G^\circ = \Delta H^\circ - T\Delta S^\circ \tag{8}$$

Using the above relationships, the thermodynamic parameters, including the standard free energy change (ΔG°), the standard enthalpy change (ΔH°), and the standard entropy change (ΔS°), were calculated and the thermodynamic parameters for this adsorption process were summarized in Table 8.

In general, the adsorption equilibrium constant K_0 decreased by increasing the solution temperature. The negative values of ΔH° verified the exothermic nature of this adsorption process and this observation also explained the decrease of adsorption capacity at higher solution temperature. The negative standard free energy changes (ΔG°) and positive standard entropy changes (ΔS°) at all temperatures indicated that the adsorption was a spontaneous process and the randomness at the solid/liquid interface during the adsorption increased dramatically. Because the size of PNA molecule is much larger than that of H_2O molecule, the adsorption of one PNA molecule at one

Table 7
The isotherm parameters of this adsorption process

	T (K)		
Parameters	278K	298K	308K
Langmuir model			
q_{max} (mg/g)	204.08	192.31	151.52
K_L (L/mg)	5.39×10^{-2}	3.93×10^{-2}	3.52×10^{-2}
R^2	0.9817	0.9920	0.9866
Δq_e (%)	7.80	5.87	7.81
Freundlich model			
$1/n$	0.6168	0.5670	0.5054
K_F ((mg/g)(L/mg)$^{1/n}$)	16.74	12.37	12.19
R^2	0.9326	0.9629	0.9861
Δq_e (%)	12.08	10.88	11.01
Redlich–Peterson model			
a	9.024	6.903	9.005
b	0.015	0.033	0.213
c	1.251	1.036	0.741
R^2	0.9936	0.9898	0.9922
Δq_e (%)	7.36	8.91	4.66
Dubinin–Radushkevich model			
q_D (mg/g)	191.6184	170.034	167.1714
B_{DR} (mol^2/kJ^2)	0.0071	0.0034	0.0092
R^2	0.9920	0.8287	0.9852
Δq_e (%)	15.78	10.54	12.90

Table 8
The thermodynamic parameters for the adsorption of PNA onto bamboo charcoal

	T (K)		
Parameters	278 K	298 K	308 K
C_s (mol/g)	1.32×10^{-2}	1.23×10^{-2}	1.14×10^{-2}
C_s^0 (mol/m^2)	1.67×10^{-5}	1.56×10^{-5}	1.45×10^{-5}
C_e (mol/L)	2.47×10^{-4}	4.34×10^{-4}	6.10×10^{-4}
K_0	3.21×10^{6}	1.82×10^{6}	1.29×10^{6}
ln K_0	14.98	14.41	14.07
ΔG° (kJ/mol)	−34.62	−35.70	−36.03
ΔH° (kJ/mol)	−14.63		
ΔS° (J/k mol)	71.91	70.70	69.48

adsorption site would inevitably push more than one H_2O molecules out of this place, so the increase of system randomness was something that must happen.

4. Conclusions

The key characteristics of commercial bamboo charcoal and the adsorption of PNA from aqueous solution by this bamboo charcoal were studied. The characteristic investigation demonstrated the complex surface morphology of bamboo charcoal and the existence of various functional groups on bamboo charcoal surface, the majority of bamboo charcoal pores fell in to the size less than 25 nm, showing the mesoporous structure was dominant on bamboo charcoal surface. The adsorption process of PNA onto bamboo charcoal was heavily affected by grain size and solution pH values, and grain size of 80–100 mesh and acidic solution pH values were proved to be optimal for the adsorption. The kinetic study revealed that the adsorption process followed pseudo-second-order model perfectly and the equilibrium data could be best fitted by the Redlich–Peterson model. The thermodynamic study showed the adsorption process was product-favored and exothermic. The change in entropy value was positive which indicated an increase in system randomness due to the replacement of H_2O molecules on the adsorption sites with PNA molecules transferred from bulk solution.

Acknowledgments

The authors would like to acknowledge financial support for this work provided by Project of the Priority Academic Program Development (PAPD) of Jiangsu Higher Education Institutions.

References

[1] S.Y. Wang, M.H. Tsai, S.F. Lo, M.J. Tsai, Effects of manufacturing conditions on the adsorption capacity of heavy metal ions by Makino bamboo charcoal, Bioresour. Technol. 99 (2008) 7027–7033.
[2] S.F. Lo, S.Y. Wang, M.J. Tsai, L.D. Lin, Adsorption capacity and removal efficiency of heavy metal ions by Moso and Ma bamboo activated carbons, Chem. Eng. Res. Des. 90 (2012) 1397–1406.
[3] F.Y. Wang, H. Wang, J.W. Ma, Adsorption of cadmium (II) ions from aqueous solution by a new low-cost adsorbent-Bamboo charcoal, J. Hazard. Mater. 177 (2010) 300–306.
[4] H. Lalhruaitluanga, K. Jayaram, M.N.V. Prasad, K.K. Kumar, Lead(II) adsorption from aqueous solutions by raw and activated charcoals of *Melocanna baccifera* Roxburgh (bamboo)—A comparative study, J. Hazard. Mater. 175 (2010) 311–318.
[5] D. Fu, Y.H. Zhang, F.z. Lv, P.K. Chu, J.W. Shang, Removal of organic materials from TNT red water by bamboo charcoal adsorption, Chem. Eng. J. 193–194 (2012) 39–49.
[6] M. Wang, Z.H. Huang, G.J. Liu, F. Kang, Adsorption of dimethyl sulfide from aqueous solution by a cost-effective bamboo charcoal, J. Hazard. Mater. 190 (2011) 1009–1015.
[7] E.L.K. Mui, W.H. Cheung, M. Valix, G. McKay, Dye adsorption onto char from bamboo, J. Hazard. Mater. 177 (2010) 1001–1005.
[8] L.G. Wang, Application of activated carbon derived from 'waste' bamboo culms for the adsorption of azo disperse dye: Kinetic, equilibrium and thermodynamic studies, J. Environ. Manage. 102 (2012) 79–87.
[9] L.S. Chan, W.H. Cheung, G. McKay, Adsorption of acid dyes by bamboo derived activated carbon, Desalination 218 (2008) 304–312.
[10] Ministry of Environmental Protection of China, China National Standard, 1989.
[11] Ministry of Environmental Protection of China, China National Standard, GB8978-1996, 1996.
[12] H.J. Ma, M. Wang, C.Y. Pu, J. Zhang, S. Zhao, S. Yao, J. Xiong, Transient and steady-state photolysis of *p*-nitroaniline in aqueous solution, J. Hazard. Mater. 165 (2009) 867–873.
[13] W.M. Wu, S.J. Liang, Y. Chen, L.J. Shen, H.R. Zheng, L. Wu, High efficient photocatalytic reduction of 4-nitroaniline to p-phenylenediamine over microcrystalline $SrBi_2Nb_2O_9$, Catal. Commun. 17 (2011) 39–42.
[14] A. Khalid, M. Arshad, D.E. Crowley, Biodegradation potential of pure and mixed bacterial cultures for removal of 4-nitroaniline from textile dye wastewater, Water Res. 43 (2009) 1110–1116.
[15] A. Qureshi, V. Verma, A. Kapley, H.J. Purohit, Degradation of 4-nitroaniline by *Stenotrophomonas* strain HPC 135, Int. Biodeterior. Biodegrad. 60 (2007) 215–218.
[16] J.H. Sun, S.P. Sun, M.H. Fan, H.Q. Guo, L.P. Qiao, R.X. Sun, A kinetic study on the degradation of p-nitroaniline by Fenton oxidation process, J. Hazard. Mater. 148 (2007) 172–177.
[17] J.H. Sun, S.P. Sun, M.H. Fan, H.Q. Guo, Y.F. Lee, R.X. Sun, Oxidative decomposition of *p*-nitroaniline in water by solar photo-Fenton advanced oxidation process, J. Hazard. Mater. 153 (2008) 187–193.
[18] K.Q. Li, Z. Zheng, J.W. Feng, J. Zhang, X. Luo, G. Zhao, X.F. Huang, Adsorption of *p*-nitroaniline from aqueous solutions onto activated carbon fiber prepared from cotton stalk, J. Hazard. Mater. 166 (2009) 1180–1185.
[19] J.H. Huang, X.G. Wang, K.L. Huang, Adsorption of p-nitroaniline by phenolic hydroxyl groups modified hyper-cross-linked polymeric adsorbent and XAD-4: A comparative study, Chem. Eng. J. 155 (2009) 722–727.
[20] K. Zheng, B.C. Pan, Q.J. Zhang, W.M. Zhang, Enhanced adsorption of p-nitroaniline from water by a carboxylated polymeric adsorbent, Sep. Purif. Technol. 57 (2007) 250–256.
[21] C.H. Geng, R.M. Cheng, X.C. Xu, Y.W. Chen, Adsorption of 4-nitroaniline and N, N-dimethylaniline on carbon nanotubes, J. East China Normal Univ. 5–6 (2008) 138–142.
[22] B.H. Hameed, M.I. El-Khaiary, Equilibrium, kinetics and mechanism of malachite green adsorption on activated carbon prepared from bamboo by K_2CO_3 activation and subsequent gasification with CO_2, J. Hazard. Mater. 157 (2008) 344–351.
[23] P. Liao, S.H. Yuan, W.J. Xie, W.B. Zhang, M. Tong, K. Wang, Adsorption of nitrogen-heterocyclic compounds on bamboo charcoal: Kinetics, thermodynamics, and microwave regeneration, J. Colloid Interface Sci. 390 (2013) 189–195.
[24] B.H. Hameed, A.T.M. Din, A.L. Ahmad, Adsorption of methylene blue onto bamboo-based activated carbon: Kinetics and equilibrium studies, J. Hazard. Mater. 141 (2007) 819–825.
[25] D.S. Zhao, J. Zhang, E.H. Duan, J. Wang, Adsorption equilibrium and kinetics of dibenzothiophene from n-octane on bamboo charcoal, Appl. Surf. Sci. 254 (2008) 3242–3247.
[26] Available from: <http://serge.engi.tripod.com/MolBio/Buffer_cal.html> (2015).
[27] M.G. Ma, X.Y. Wei, H.G. Zhao, Study of preparation of modified bentonite and its adsorption of nitroaniline, Environ. Eng. 30 (2012) 317–321.
[28] L. Yang, H.B. Liu, D.S. Zhao, J. Liu, Electron microscopy study on microstructure of bamboo charcoal, J. Chin. Electr. Microsc. Soc. 30 (2011) 137–142.
[29] P. Chingombe, B. Saha, R.J. Wakeman, Surface modification and characterisation of a coal-based activated carbon, Carbon 43 (2005) 3132–3143.
[30] Q.S. Liu, T.Z. Zheng, P. Wang, L. Guo, Preparation and characterization of activated carbon from bamboo by microwave-induced phosphoric acid activation, Ind. Crops. Prod. 31 (2009) 233–238.
[31] H.C. Huang, D.Q. Ye, B.C. Huang, Nitrogen plasma modification of viscose-based activated carbon fibers, Surf. Coat. Technol. 201 (2007) 9533–9540.

[32] S. Kodama, H. Habaki, H. Sekiguchi, J. Kawasaki, Surface modification of adsorbents by dielectric barrier discharge, Thin Solid Films 407 (2002) 151–155.
[33] S. Kondo, T. Ishikawa, I. Abe, Science of Adsorption, Maruzen Publishers Inc., Tokyo, 1991.
[34] G.H. Chen, Applied Physical Chemistry, Chemical Industrial Press, Beijing, 2008.
[35] G.Q. Wu, X.Y. Zhang, H. Hui, J. Yan, Q.S. Zhang, J.L. Wan, Y. Dai, Adsorptive removal of aniline from aqueous solution by oxygen plasma irradiated bamboo based activated carbon, Chem. Eng. J. 185–186 (2012) 201–210.
[36] F.C. Wu, B.L. Liu, K.T. Wu, A new linear form analysis of Redlich–Peterson isotherm equation for the adsorptions of dyes, Chem. Eng. J. 162 (2010) 21–27.
[37] H. Al-Johani, M.A. Salam, Kinetics and thermodynamic study of aniline adsorption by multi walled carbon nanotubes from aqueous solution, J. Colloid Interface Sci. 360 (2011) 760–767.
[38] M.A. Salama, R.C. Burk, Thermodynamics of pentachlorophenol adsorption from aqueous solutions by oxidized multi-walled carbon nanotubes, Appl. Surf. Sci. 255 (2008) 1975–1981.